*Journal of Sound and Vibration* (1998) **214**(3), 443–467
*Article No*. sv981574

# ON THE VIBRATION FIELD CORRELATION OF RANDOMLY EXCITED FLAT PLATE STRUCTURES, I: THEORY

M. W. Bonilha† and F. J. Fahy

*Institute of Sound and Vibration Research, University of Southampton, Highfield, Southampton, SO17 1BJ, England*

(*Received* 6 *May* 1997, *and in final form* 26 *January* 1998)

A probabilistic treatment of the vibration field generated by the random vibration of flat plate components is proposed herein. This treatment is based on the computation of the frequency-averaged spatial correlation coefficient of the plate normal displacement. This spatial correlation coefficient is derived using an approximate modal representation based on Bolotin's Method of Integral Estimates. Particular attention is paid to the boundary conditions and results are derived for plates with clamped, simply supported, free or guided edges. A general boundary condition which solely depends on the edge stiffness is employed to model the effect of stiffeners on the plate vibration field. Information about the type of excitation is also incorporated in this model. This approximate representation is compared to that obtained by a modal summation method and good agreement between both approaches is obtained for cases in which at least eight modes are resonant in a frequency band.



## 1. INTRODUCTION

The dynamic response of a plate-like structural component due to random excitation can be resolved in terms of its normal modes of vibration. Such a solution involves the "exact" determination of the plate natural modes of vibration and associated natural frequencies. Deterministic approaches such as the Finite Element Method (FEM) are well established for the solution of this dynamic problem. However, the sensitivity of modal resonance frequencies and relative modal phase response to small variations in structural detail increase with modal order and, as a result, deterministic methods such as the FEM are unreliable for the exact computation of the random response of dynamic systems involving high order modes.

This stems from the fact that it is impossible to compute the precise spatial distribution of amplitude and phase of a vibrational field involving high order modes because these modes are very sensitive to damping distributions, joints and other boundary conditions, about which there is always significant uncertainty. Moreover, deterministic computation must be carried out frequency by frequency, and the response results are then normally compiled in frequency bands, which implies that a large amount of data is unnecessarily processed.

On the other hand, probabilistic methods based on power flow equations such as Statistical Energy Analysis (SEA) are more appropriate for solving this problem in cases

† Now at United Technologies Research Center, 411 Silver Lane, East Hartford, CT 06108, U.S.A.

0022–460X/98/280443 + 25 $30.00/0 

in which the structural system under study is modally dense. However, SEA does not provide information about the actual spatial distribution of the vibration velocity field set up in structural components under random excitation.

An approximate description is proposed herein for the spatial response distribution of the bending wave field generated by the random vibration of thin plate-like structural components. This representation is based on the computation of spatial correlation characteristics of the vibration field, which are described by a frequency averaged parameter, the zero time delay spatial correlation coefficient of the plate response.

As discussed by Maidanik [1], the form of the correlation field, specially near the edges and perturbations, is very important for the prediction of the sound radiation of plane structures below the critical frequency. In reference [1], Maidanik uses the spatial correlation of a single mode of a simply-supported plate to estimate the radiation efficiency of this mode. The single mode result was then employed to generate an estimate for the acoustic radiation efficiency of a modally dense plate whose vibration field is reverberant.

The expressions for the multi-modal spatial correlation coefficient presented herein enable the band limited acoustic radiation efficiency of plane structures to be computed directly without resorting to investigation of the single mode radiation efficiency or without the necessity of precise determination of the structural modes [2]. In addition, as described in reference [2], the vibroacoustic coupling between a modally dense plate and a modally sparse acoustic cavity can also be estimated based on the expressions derived in this work. This type of interaction model is very important to interior noise control in transportation vehicles. In both cases, the use of a band limited representation is very convenient as it avoids the impractical frequency-by-frequency computation of the plate response and associated acoustic radiation. Finally, it can also be pointed out that band-limited estimates of the dynamic stress/strain concentrations near the boundaries of flat plate structures could also be computed by substituting the expressions derived in this work in the analysis presented in reference [3].

Asymptotic expressions for the spatial distribution of the mean square vibration velocity of point excited simply-supported rectangular and square plates under wide band random excitation were derived by Crandall [4, 5] using the method of images. The lines of intensified response predicted by these asymptotic expressions have been observed in square, rectangular, circular and triangular plates using salt grains spread over the plates surface. These lines of intensified response pass along specific lines dictated by the position of the excitation force and plate geometry. Under the assumption of wide band random excitation the expressions presented herein closely approximate to those derived by Crandall [4, 5].

For other types of excitation the method of integral estimates proposed by Bolotin [6] provides useful information on the wide band response of structural systems. In this method summation over mode shapes, modal damping, excitation cross-spectral densities are substituted by integration over wavenumber space assuming these functions are slowly varying in the wavenumber space. Application of this method to practical structures enabled the derivation of wide-band expressions for the correlation functions and spectral densities of the displacements, stress and strains of plates under random forces [6, 7].

In what follows, the response of flat plates to spatially uncorrelated forces is represented using approximate mode shapes obtained by Bolotin's Asymptotic Method (also called the Dynamic Edge Effect Method) [6]. These approximate mode shapes are used to derive frequency averaged spatial correlation coefficients of the response of plates with simply supported, clamped, free, guided or spring supported edges. Approximations are also given for the case of point excited plates or plates driven by acoustic excitation in the form of

a diffuse acoustic field. The closed form result derived for plates with all around simply supported edges is then compared with results obtained by a standard modal summation method.

## 2. CORRELATION COEFFICIENTS OF RANDOM PROCESSES

Consider a continuous, time-invariant, linear system subjected to stationary random excitation. The displacements, ($z_1(\mathbf{x}_1, t)$ and $z_2(\mathbf{x}_2, t)$), at two different positions in this system can be considered to be stationary random processes. Thus, the cross-correlation function between the system displacements at points 1 and 2 is defined as [8]

$$R_{12}(\mathbf{x}_1, \mathbf{x}_2, \tau) = E[z_1(\mathbf{x}_1, t) z_2(\mathbf{x}_2, t+\tau)], \tag{1}$$

where $E[\ ]$ represents the expected value, or the ensemble averaged value, of the quantity in square brackets, and $\tau$ is the time delay between the two signals.

Assuming that the random process $z_1$ and $z_2$ have zero mean value, the cross-correlation coefficient (or normalized covariance), $\gamma_{12}(\mathbf{x}_1, \mathbf{x}_2, \tau)$, for these random processes can be written as [8]

$$\gamma_{12}(\mathbf{x}_1, \mathbf{x}_2, \tau) = R_{12}(\mathbf{x}_1, \mathbf{x}_2, \tau)/(E[z_1^2(\mathbf{x}_1, t)])^{1/2}(E[z_2^2(\mathbf{x}_2, t)])^{1/2}, \tag{2}$$

where $E[z_1^2]$ and $E[z_2^2]$ are the mean square values of the random processes $z_1$ and $z_2$, respectively.

Using the Wiener–Khinchin relationship one can relate the cross-correlation function with the cross-power spectral density

$$R_{12}(\mathbf{x}_1, \mathbf{x}_2, \tau) = \mathrm{Re}\left[\int_0^\infty G_{12}(\mathbf{x}_1, \mathbf{x}_2, f) \exp(\mathrm{i}2\pi f\tau)\, \mathrm{d}f\right], \tag{3}$$

where $G_{12}(\mathbf{x}_1, \mathbf{x}_2, f)$ is the one-sided cross-power spectral density of random variable $z$ at positions 1 and 2.

For $\tau = 0$, equation (3) yields

$$R_{12}(\mathbf{x}_1, \mathbf{x}_2, \tau = 0) = \int_0^\infty \mathrm{Re}\,[G_{12}(\mathbf{x}_1, \mathbf{x}_2, f)\, \mathrm{d}f. \tag{4}$$

The contribution of frequency components of $G_{12}(\mathbf{x}_1, \mathbf{x}_2, f)$ in a finite frequency band $\Delta f$ is obtained by the integration of this function between $f_2$ and $f_1$, where $f_2$ and $f_1$ are the upper and lower frequency limits of the band $\Delta f$. Hence, in a frequency band the corresponding zero-time delay spatial correlation coefficient can be termed the frequency averaged spatial correlation coefficient ($\gamma_{12}(\mathbf{x}_1, \mathbf{x}_2, f_c)$), where $f_c$ is the band centre frequency and the explicit indication of zero time delay is dropped for convenience. The mean square value of the random processes $z_1$ and $z_2$ in a frequency band ($f_1 - f_2$) can be obtained from

$$E[z_1^2(\mathbf{x}_1, t)] = \int_{f_1}^{f_2} G_1(f)\, \mathrm{d}f, \qquad E[z_2^2(\mathbf{x}_2, t)] = \int_{f_1}^{f_2} G_2(f)\, \mathrm{d}f, \tag{5}$$

where $G_1(f)$ and $G_2(f)$ are the auto-spectral densities of the random processes $z_1$ and $z_2$ at positions 1 and 2, respectively.

Thus, from equations (5), (4) and (2), in a given frequency band, one has

$$\gamma_{12}(\mathbf{x}_1, \mathbf{x}_2, f_c) = \int_{f_1}^{f_2} \mathrm{Re}\,[G_{12}(\mathbf{x}_1, \mathbf{x}_2, f)]\,\mathrm{d}f \Big/ \left[\int_{f_1}^{f_2} G_1(f)\,\mathrm{d}f\right]^{1/2} \left[\int_{f_1}^{f_2} G_2(f)\,\mathrm{d}f\right]^{1/2}. \tag{6}$$

The above equation is convenient for experimental computation of spatial correlation coefficient values and it was extensively utilised in the experimental work reported in a companion paper [9]. Moreover, this equation is equivalent to the correlation density coefficient as defined by Morrow [10] and employed in the analysis of correlation of sound pressures in reverberant sound fields.

Equation (6) can also be employed in the theoretical derivation of frequency averaged spatial correlation coefficients based on a modal model as described in section 5. Alternatively, a different procedure can be employed in the computation of the spatial correlation coefficient using a modal model. The modal spatial correlation coefficient when one single undamped mode is present is given by [10]

$$\gamma_{12M}(\mathbf{x}_1, \mathbf{x}_2) = \langle z_{1M}(t) z_{2M}(t)\rangle_t / [\langle z_{1M}^2(t)\rangle_t]^{1/2} [\langle z_{2M}^2(t)\rangle_t]^{1/2}, \tag{7}$$

where $z_{1M}(t)$ and $z_{2M}(t)$ are the instantaneous modal displacements at positions 1 and 2, and $\langle\ \rangle_t$ represents time averaging of the quantity inside the brackets. In the above coefficient, the specific mode numbers $k_x$ and $k_y$ are represented by an intersection of the lines of the grid shown in Figure 1. As the time dependence of an undamped vibration mode is expressed by a sinusoidal factor the modal correlation coefficient equals $\pm 1$ [10].

In a frequency band in which more than one mode is present, the frequency averaged correlation coefficient can be obtained by summing the contribution from all modes that have resonance frequencies in this band. In addition, assuming that these modes are uncorrelated one can write the frequency averaged correlation coefficient as

$$\gamma_{12}(\mathbf{x}_1, \mathbf{x}_2, f_c) = \sum_N \langle z_{1M}(t) z_{2M}(t)\rangle_t \Big/ \left[\sum_N \langle z_{1M}^2(t)\rangle_t\right]^{1/2} \left[\sum_N \langle z_{2M}^2(t)\rangle_t\right]^{1/2}. \tag{8}$$

Alternatively, if the density of modal frequencies is high, the number of modes (N) summed in equation (8) is large and the summation can be converted into integration over wavenumber space [6]. The limits of integration are for an interval $\Delta k$ around $k_b$, the bending wavenumber of the centre frequency of the band (Figure 1). Equation (8) becomes

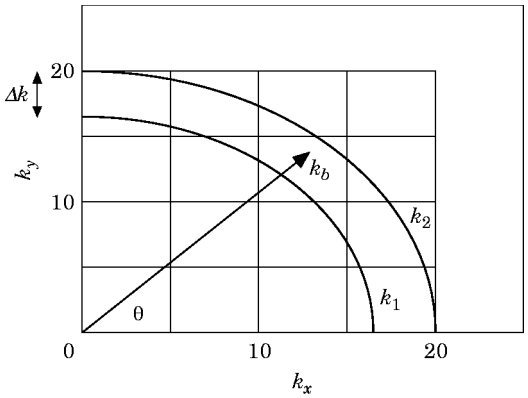


Figure 1. Grid of discrete modes compared with continuous function representation in terms of $k_b$ and $\theta$.

$$\gamma_{12}(\mathbf{x}_1, \mathbf{x}_2, f_c) = \int_{\Delta k} \langle\langle z_{1M}(t) z_{2M}(t)\rangle_t \rangle \, \mathrm{d}k_B \Big/ \left[\int_{\Delta k} \langle\langle z_{1M}^2(t)\rangle_t \rangle \, \mathrm{d}k_B\right]^{1/2} \times \left[\int_{\Delta k} \langle\langle z_{2M}^2(t)\rangle_t \rangle \, \mathrm{d}k_B\right]^{1/2}, \tag{9}$$

where $\langle\ \rangle$ denotes an average over a quarter circle of radius $k_B$ in the wavenumber space. Changing from rectangular to cylindrical co-ordinates it follows that $k_x = k_B \cos\theta$ and $k_y = k_B \sin\theta$ (Figure 1). As a result, the frequency averaged spatial correlation coefficient can be obtained from

$$\gamma_{12}(\mathbf{x}_1, \mathbf{x}_2, f_c) = \int_{\Delta k}\int_0^{\pi/2} [\langle z_{1M}(t) z_{2M}(t)\rangle_t] \, \mathrm{d}\theta \, \mathrm{d}k_B \Big/ \left[\int_{\Delta k}\int_0^{\pi/2} \langle z_{1M}^2(t)\rangle_t \, \mathrm{d}\theta \, \mathrm{d}k_B\right]^{1/2} \times \left[\int_{\Delta k}\int_0^{\pi/2} \langle z_{2M}^2(t)\rangle_t \, \mathrm{d}\theta \, \mathrm{d}k_B\right]^{1/2}. \tag{10}$$

## 3. SPATIAL CORRELATION COEFFICIENTS ON MODALLY DENSE SIMPLY SUPPORTED FLAT PLATES

The contribution of $N$ vibration modes to normal displacement response of a simply supported flat plate is given by

$$z(x, y, t) = \sum_{M=1}^{N} \sin(k_{xM} x) \sin(k_{yM} y) Z_M(t), \tag{11}$$

where $k_{xM}$ and $k_{yM}$ are the modal bending wavenumbers in the $x$ and $y$ directions and $Z_M(t)$ represents the modal time dependence. The displacements at points 1 and 2 for one particular mode are

$$z_{1M}(t) = Z_M(t) \sin(k_{xM} x_1) \sin(k_{yM} y_1),$$
$$z_{2M}(t) = Z_M(t) \sin(k_{xM} x_2) \sin(k_{yM} y_2), \tag{12}$$

where $(x_1, y_1)$ and $(x_2, y_2)$ are co-ordinates of points 1 and 2 as illustrated in Figure 2.

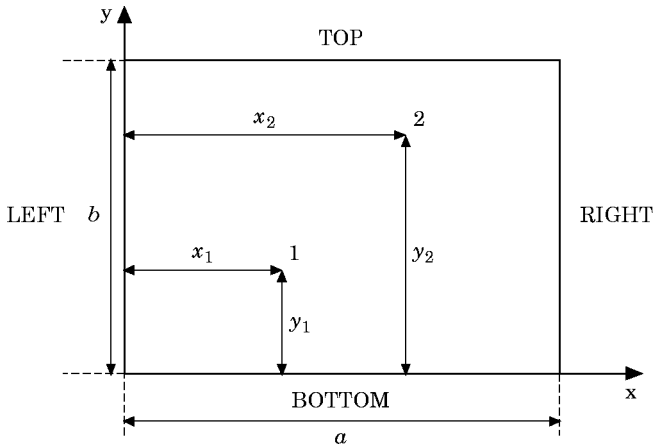


Figure 2. Sketch of plate used in the derivation of spatial correlation coefficients.

Multiplying and time averaging the displacements at points 1 and 2 one has

$$\langle z_{1M}(t) z_{2M}(t)\rangle_t = \overline{Z_M^2} \sin(k_{xM} x_1) \sin(k_{xM} x_2) \sin(k_{yM} y_1) \sin(k_{yM} y_2), \tag{13}$$

where $\overline{Z_M^2}$ is the mean square value of $Z_M(t)$. Using standard trigonometric transformations it follows from equation (13) that

$$\begin{aligned}\langle z_{1M}(t) z_{2M}(t)\rangle_t = \overline{Z_M^2}\,[1/2(\cos(k_{xM}(x_1 - x_2)) - \cos(k_{xM}(x_1 + x_2)))] \\ \times [1/2(\cos(k_{yM}(y_1 - y_2)) - \cos(k_{yM}(y_1 + y_2)))].\end{aligned} \tag{14}$$

Following the procedure suggested in section (2) $k_{xM}$ and $k_{yM}$ can be expressed in terms of the bending wavenumber ($k_B$) and angle $\theta$. The sum over the individual modes is then substituted by an integration carried out in a strip of width $\Delta k$ much smaller than the band centre frequency wavenumber ($k_b$) (illustration in Figure 1). This substitution is the basis of the method of integral estimates as proposed by Bolotin [6]. The result of this operation is

$$\begin{aligned}\sum_{M \in \Delta k} \langle z_{1M}(t) z_{2M}(t)\rangle_t &= \int_{\Delta k}\int_0^{\pi/2} \langle z_{1M}(t) z_{2M}(t)\rangle_t \,\mathrm{d}\theta\,\mathrm{d}k_B \\ &= \frac{N\overline{Z_M^2}}{4}\int_{\Delta k}\Bigg[\int_0^{\pi/2} \cos(k_B(x_1 - x_2)\cos\theta)\cos(k_B(y_1 - y_2)\sin\theta)\,\mathrm{d}\theta \\ &\quad - \int_0^{\pi/2} \cos(k_B(x_1 - x_2)\cos\theta)\cos(k_B(y_1 + y_2)\sin\theta)\,\mathrm{d}\theta \\ &\quad - \int_0^{\pi/2} \cos(k_B(x_1 + x_2)\cos\theta)\cos(k_B(y_1 - y_2)\sin\theta)\,\mathrm{d}\theta \\ &\quad + \int_0^{\pi/2} \cos(k_B(x_1 + x_2)\cos\theta)\cos(k_B(y_1 + y_2)\sin\theta)\,\mathrm{d}\theta\Bigg]\mathrm{d}k_B,\end{aligned} \tag{15}$$

where $N$ modes are assumed to be excited in the band $\Delta k$ and $\overline{Z_M^2}$ is assumed equal for all modes. The four integrals inside the brackets in the above equation can be solved using equation (A3) presented in Appendix A. The solution is

$$\begin{aligned}\frac{\pi}{2}[\mathrm{J}_0(k_B\sqrt{(x_1 - x_2)^2 + (y_1 - y_2)^2}) - \mathrm{J}_0(k_B\sqrt{(x_1 - x_2)^2 + (y_1 + y_2)^2}) \\ - \mathrm{J}_0(k_B\sqrt{(x_1 + x_2)^2 + (y_1 - y_2)^2}) + \mathrm{J}_0(k_B\sqrt{(x_1 + x_2)^2 + (y_1 + y_2)^2})].\end{aligned} \tag{16}$$

The expressions for $\int_0^{\pi/2}\langle z_{1M}^2(t)\rangle_t\,\mathrm{d}\theta$ and $\int_0^{\pi/2}\langle z_{2M}^2(t)\rangle_t\,\mathrm{d}\theta$ can be obtained from equations (15) and (16) by making $x_1 = x_2$ and $y_1 = y_2$. The resulting integrals can then be solved using expressions (A1), (A2) and (A3) from Appendix A. For point 1 the result is

$$\int_0^{\pi/2}\langle z_{1M}^2(t)\rangle_t\,\mathrm{d}\theta = \frac{N\pi\overline{Z_M^2}}{8}[1 - \mathrm{J}_0(2k_B x_1) - \mathrm{J}_0(2k_B y_1) + \mathrm{J}_0(2k_B\sqrt{x_1^2 + y_1^2})]. \tag{17}$$

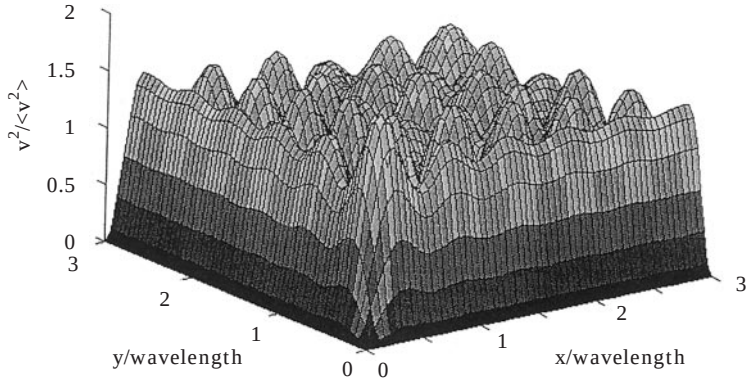


Figure 3. Interference patterns near the corner of a simply supported plate.

When divided by $N\pi\overline{Z_M^2}/8$, the above expression gives the interference patterns near the boundaries of the plate as originally derived by Lyon [11]. It expresses the relation between the mean square acceleration near the boundaries and its equivalent in a position far from the boundaries. A sketch of such interference patterns near the corner of a plate are presented in Figures 3 and 4. They are sketched as a function of a typical wavelength ($\lambda$) and it can be noted from the contour plot of Figure 4 that when $x_1, y_1 \geqslant \lambda$ and $x_2, y_2 \geqslant \lambda$ the mean square values of the response variable do not depart considerably from the spatial average ($\langle v^2 \rangle$).

The integral of the type

$$\int_{k_1}^{k_2} \mathrm{J}_0\,(k_B\, r)\,\mathrm{d}k_B, \tag{18}$$

required when the terms of equation (16) and (17) are summed in the strip $\Delta k = k_1 - k_2$, has been shown by Cook *et al*. [12] to be given by

$$\mathrm{J}_0\,(k_b\, r)\Delta k + \text{terms of the order } ((k_2 - k_1)/k_b)^2 \Delta k \tag{19}$$

where $k_b$ is the bending wavenumber at the band centre frequency. Assuming that the width of the strip is small enough for the second terms in equation (19) to be neglected, one obtains from equations (15)–(17) and (10) an approximate expression for the frequency

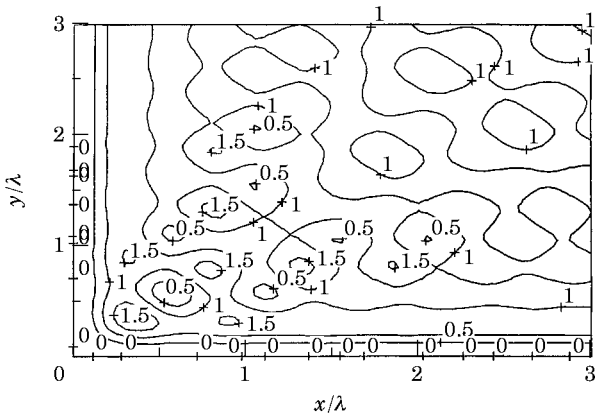


Figure 4. Contour plot for the interference patterns near the corner of a simply supported flat plate.

averaged spatial correlation coefficient of vibration displacement between two points on a simply supported homogeneous flat plate. This expression is,

$$\gamma_{12}(\mathbf{x}_1, \mathbf{x}_2, f_c) = \frac{\begin{array}{c}[\mathrm{J}_0(k_b\sqrt{(x_1-x_2)^2+(y_1-y_2)^2}) - \mathrm{J}_0(k_b\sqrt{(x_1-x_2)^2+(y_1+y_2)^2})\\ -\mathrm{J}_0(k_b\sqrt{(x_1+x_2)^2+(y_1-y_2)^2}) + \mathrm{J}_0(k_b\sqrt{(x_1+x_2)^2+(y_1+y_2)^2})]\end{array}}{\begin{array}{c}[1-\mathrm{J}_0(2k_b x_1) - \mathrm{J}_0(2k_b y_1) + \mathrm{J}_0(2\mathrm{k_b}\sqrt{x_1^2+y_1^2})]^{1/2}\\ \times[1 - J_0(2k_b x_2) - \mathrm{J}_0(2k_b y_2) + \mathrm{J}_0(2k_b\sqrt{x_2^2+y_2^2})]^{1/2}\end{array}}. \quad (20)$$

The above result is valid in frequency bands whose centre frequency is $f_c$ (with corresponding bending wavenumber $k_b$) in which a spatially uncorrelated random source excites a large number of plate modes. As the bandwidth of the frequency band increases beyond a certain limit the frequency averaged coefficient presented in equation (20) is no longer valid. Equation (20) is also valid for the frequency averaged spatial correlation coefficient of vibration velocity or acceleration on simply supported plates.

All the results presented in this section presuppose that points 1 and 2 are situated in the quarter space bounded by $0 \leqslant x \leqslant a/2$ and $0 \leqslant y \leqslant b/2$, where $a$ and $b$ are the plate dimensions (Figure 2). However, they are unaffected by the substitution $x \rightarrow a\text{-}x$, $y \rightarrow b\text{-}y$ (p. 121, reference [11]) and, therefore can be used to represent the interference patterns and correlation coefficients in other sections of the plate.

A number of simplifications can be carried out in equation (20) but the most important one is for the case in which points 1 and 2 are far from the edges. In this situation, the three last terms on the right side of equation (17) and on equation (16) approach zero and are much smaller than the first term. For this reason, these terms can be neglected. As a result, one obtains equation (21) which gives the frequency averaged spatial correlation coefficient in points remote from the edges on a simply supported flat plate.

$$\gamma_{12}(\mathbf{x}_1, \mathbf{x}_2, f_c) = \mathrm{J}_0(k_b r), \quad (21)$$

where $r$ is the distance between points 1 and 2. However, this approximation is not valid for some specific lines in which there is superposition of nodal lines. This is the result derived by Cook *et al*. [12] and by Morrow [10] for a two-dimensional reverberant sound field. Similarly, Stearn [13] has shown that this result also applies to a diffuse bending wave field provided that the frequency band is restricted to a one-third octave and $k_b r$ is less than ten. Even though the present analysis has been restricted to simply supported edges, equation (21) is valid for any type of boundary condition because, as shown by Bolotin [6], flat structures behave like simply supported plates at points remote from their boundaries at frequencies high compared with the fundamental resonance frequency.

## 4. SPATIAL CORRELATION COEFFICIENTS ON MODALLY DENSE FLAT PLATES WITH GENERIC BOUNDARY CONDITIONS

In order to derive an expression for the spatial correlation coefficients of the vibration response of random excited flat plates with arbitrary boundary conditions, the dynamic response of a rectangular plate is represented using Bolotin's dynamic edge effect method [6]. This method involves using a generating (inner) solution in the form of a sinusoidal function and an exponential term (outer solution) that accounts for the dynamic boundary effect in the boundary zone. For the case of a rectangular plate in which the edges generate an evanescent near field, an approximate representation for the normal displacements at points 1 and 2 for one particular resonant mode can be written as [6]

$$z_{1M}(t) = Z_M(t)X(x_1)Y(y_1), \qquad z_{2M}(t) = Z_M(t)X(x_2)Y(y_2), \quad (22)$$

where,

$$X(x) = \sin k_x (x - \xi_x) + C_x \exp(-\mu_x x), \qquad Y(y) = \sin k_y (y - \xi_y) + C_y \exp(-\mu_y y),$$
$$\mu_x = \sqrt{k_x^2 + 2k_y^2}, \qquad \mu_y = \sqrt{k_y^2 + 2k_x^2}.$$

The dynamic edge parameters, $\sin k_x \xi_x$, $\cos k_x \xi_x$, $C_x, \cos k_y \xi_y$, $\sin k_y \xi_y$, $C_y$, are obtained from the plate boundary conditions. The dynamic edge parameters for simply supported, clamped, free, guided or spring supported edges are presented in Appendix B. Multiplying and time averaging the displacements at points 1 and 2 one obtains expressions for $\langle z_{1M}(t) z_{2M}(t)\rangle_t$, $\langle z_{1M}^2(t)\rangle_t$ and $\langle z_{2M}^2(t)\rangle_t$. These expressions are valid for a single mode with modal wavenumbers $k_x$ and $k_y$. As already presented, a frequency averaged value for these expressions can be obtained by summing the contribution from each mode that is excited in the band. Alternatively, when the structure has a high modal density the discrete wavenumbers $(k_{xM}, k_{yM})$ can be substituted by the continuous functions $k_B \cos\theta$ and $k_B \sin\theta$ and the modal summation substituted by an integration over wavenumber space (Figure 1). In addition, the dynamic edge parameters will also be function of $k_B$ and $\theta$, though this dependence is omitted in equations (23) to (28).

Performing this substitution one has that

$$\sum_{M \in \Delta k} \langle z_{1M}(t) z_{2M}(t)\rangle_t = \int_{\Delta k} \int_0^{\pi/2} \langle z_{1M}(t) z_{2M}(t)\rangle_t \, \mathrm{d}\theta \, \mathrm{d}k_B$$
$$= N\overline{Z_M^2} \int_{\Delta k} \int_0^{\pi/2} X(x_1) X(x_2) Y(y_1) Y(y_2) \, \mathrm{d}\theta \, \mathrm{d}k_B, \tag{23}$$

where,

$$\begin{aligned} X(x_1)X(x_2) = {} & \tfrac{1}{2}[\cos(k_B (x_1 - x_2)\cos\theta) - \cos(k_B (x_1 + x_2)\cos\theta)\cos(2\xi_x k_B \cos\theta) \\ & - \sin(k_B (x_1 + x_2)\cos\theta)\sin(2\xi_x k_B \cos\theta)] + C_x^2 \exp(-\mu_x (x_1 + x_2)) \\ & + C_x \exp(-\mu_x x_2)[\cos(\xi_x k_B \cos\theta)\sin(k_B x_1 \cos\theta) \\ & + \sin(\xi_x k_B \cos\theta)\cos(k_B x_1 \cos\theta)] \\ & + C_x \exp(-\mu_x x_1)[\cos(\xi_x k_B \cos\theta)\sin(k_B x_2 \cos\theta) \\ & + \sin(\xi_x k_B \cos\theta)\cos(k_B x_2 \cos\theta)], \end{aligned} \tag{24}$$

and

$$\begin{aligned} Y(y_1)Y(y_2) = {} & \tfrac{1}{2}[\cos(k_B (y_1 - y_2)\sin\theta) - \cos(k_B (y_1 + y_2)\sin\theta)\cos(2\xi_y k_B \sin\theta) \\ & - \sin(k_B (y_1 + y_2)\sin\theta)\sin(2\xi_y k_B \sin\theta)] + C_y^2 \exp(-\mu_y (y_1 + y_2)) \\ & + C_y \exp(-\mu_y y_2)[\cos(\xi_y k_B \sin\theta)\sin(k_B y_1 \sin\theta) \\ & + \sin(\xi_y k_B \sin\theta)\cos(k_B y_1 \sin\theta)] \\ & + C_y \exp(-\mu_y y_1)[\cos(\xi_y k_B \sin\theta)\sin(k_B y_2 \sin\theta) \\ & + \sin(\xi_y k_B \sin\theta)\cos(k_B y_2 \sin\theta)], \end{aligned} \tag{25}$$

and $N$ modes are assumed to be excited in the band $\Delta k$. In order to estimate the correlation coefficient, analytical expressions for $\Sigma_{M \in \Delta k} \langle z_{1M}^2(t)\rangle_t$ and $\Sigma_{M \in \Delta k} \langle z_{2M}^2(t)\rangle_t$ are

also needed. These expressions are obtained from (23) by setting $x_1 = x_2$ and $y_1 = y_2$. For point 1 one has that

$$\sum_{M \in \Delta k} \langle z_{1M}^2(t) \rangle_t = \int_{\Delta k} \int_0^{\pi/2} \langle z_{1M}^2(t) \rangle_t \, \mathrm{d}\theta \, \mathrm{d}k_B = N\overline{Z_M^2} \int_{\Delta k} \int_0^{\pi/2} W(x_1) W(x_2) \, \mathrm{d}\theta \, \mathrm{d}k_B, \quad (26)$$

where

$$\begin{aligned} W(x_1) = {} & \tfrac{1}{2}[1 - \cos(2k_B x_1 \cos\theta) \cos(2\xi_x k_B \cos\theta) - \sin(2k_B x_1 \cos\theta) \sin(2\xi_x k_B \cos\theta)] \\ & + 2C_x \exp(-\mu_x x_1)[\cos(\xi_x k_B \cos\theta) \sin(k_B x_1 \cos\theta) \\ & + \sin(\xi_x k_B \cos\theta) \cos(k_B x_1 \cos\theta)] + C_x^2 \exp(-2\mu_x x_1). \end{aligned} \quad (27)$$

and,

$$\begin{aligned} W(y_1) = {} & \tfrac{1}{2}[1 - \cos(2k_B y_1 \sin\theta) \cos(2\xi_y k_B \sin\theta) - \sin(2k_B y_1 \sin\theta) \sin(2\xi_y k_B \sin\theta)] \\ & + 2C_y \exp(-\mu_y y_1)[\cos(\xi_y k_B \sin\theta) \sin(k_B y_1 \sin\theta) \\ & + \sin(\xi_y k_B \sin\theta) \cos(k_B y_1 \sin\theta)] + C_y^2 \exp(-2\mu_y y_1). \end{aligned} \quad (28)$$

The expression for $\sum_{M \in \Delta k} \langle z_{2M}^2(t) \rangle_t$ is analogous to (26) with the index 1 substituted by 2 in expressions (27) and (28). In the above expressions one has that,

$$\mu_x = k_B \sqrt{1 + \sin^2\theta}, \qquad \mu_y = k_B \sqrt{1 + \cos^2\theta}. \quad (29)$$

Finally, from (10), (23) and (26) one obtains an expression for the frequency averaged spatial correlation coefficient at points $\mathbf{x}_1 = (x_1, y_1)$ and $\mathbf{x}_2 = (x_2, y_2)$,

$$\gamma_{12}(\mathbf{x}_1, \mathbf{x}_2, f_c) = \frac{\displaystyle\int_{\Delta k} \int_0^{\pi/2} X(x_1) X(x_2) Y(y_1) Y(y_2) \, \mathrm{d}\theta \, \mathrm{d}k_B}{\left[\displaystyle\int_{\Delta k} \int_0^{\pi/2} W(x_1) W(y_1) \, \mathrm{d}\theta \, \mathrm{d}k_B\right]^{1/2} \left[\displaystyle\int_{\Delta k} \int_0^{\pi/2} W(x_2) W(y_2) \, \mathrm{d}\theta \, \mathrm{d}k_B\right]^{1/2}}, \quad (30)$$

where $X(x_1)X(x_2)$, $Y(y_1)Y(y_2)$, $W(x_1)$, $W(y_1)$, $W(x_2)$ and $W(y_2)$ are given by equations (24), (25), (27), (28).

The above result allows the computation of spatial correlation coefficients for different types of boundary conditions by using the relevant dynamic edge parameters which are presented in Appendix B. For the majority of these boundary conditions the integration in wavenumber space has to be performed numerically, since no closed form solutions have been found for these integrals. Attempts were made to obtain closed form expressions using various integration procedures, results from tables of integrals [14], and symbolic languages such as Maple V. However, no computationally convenient expressions were found for the correlation coefficient of plates with clamped, free or spring supported edges. Therefore, one had to resort to numerical integration as a means of computing the correlation coefficient of plates with these boundary conditions. Nevertheless, as the integration in angle $\theta$ is performed in only one variable the computing time involved is not critical. The numerical efficiency and precision aspects of the integration routines employed are discussed in reference [2].

Similar results can also be derived using a free wave approach [15] as presented in reference [2]. The use of the free wave approach also enables the derivation of results for plates with edges with different boundary conditions, such as a plate with two simply supported edges and two free edges. The analytical results derived herein are compared with experimental results of frequency averaged spatial correlation coefficients obtained on various plates in a companion paper [9].

## 5. INFLUENCE OF ACOUSTIC AND MECHANICAL EXCITATION ON THE SPATIAL CORRELATION COEFFICIENT

Assuming the plate natural modes of vibration are available, the cross-spectrum of the normal vibration acceleration on a flat plate excited by a random field of cross-spectrum $S_1(\epsilon_1, \xi_1, \epsilon_2, \xi_2, \omega)$ can be written as [16],

$$S_a(x_1, y_1, x_2, y_2, \omega) = \omega^4 \sum_p \sum_q \frac{\phi_p(x_1, y_1)\phi_q(x_2, y_2)}{M_p M_q} \frac{[H_p - iW_p]}{[H_p^2 + W_p^2]} \frac{[H_q + iW_q]}{[H_q^2 + W_q^2]} \times \int_S \int_S S_f(\epsilon_1, \xi_1, \epsilon_2, \xi_2, \omega)\phi_p(\epsilon_1, \xi_1)\phi_q(\epsilon_2, \xi_2)\, d\epsilon_1\, d\epsilon_2\, d\xi_1\, d\xi_2, \tag{31}$$

where $\phi_p(x_1, y_1)$ represents the mode shape of the $p$th plate mode with natural frequency $\omega_p$ at point 1, $\eta_p$ is the modal loss factor, $M_p$ is the modal mass, $H_p = \omega_p^2 - \omega^2$ and $W_p = \eta_p \omega\, \omega_p$. When the modal overlap factor is very much smaller than unity the cross terms do not contribute significantly to the response and can be neglected. Expression (31) is then written as

$$S_a(x_1, y_1, x_2, y_2, \omega) = \omega^4 \sum_p \frac{\phi_p(x_1, y_1)\phi_p(x_2, y_2)}{\Delta_p^2} \frac{1}{[H_p^2 + W_p^2]} \times \int_S \int_S S_f(\epsilon_1, \xi_1, \epsilon_2, \xi_2, \omega)\phi_p(\epsilon_1, \xi_1)\phi_p(\epsilon_2, \xi_2)\, d\epsilon_1\, d\epsilon_2\, d\xi_1\, d\xi_2. \tag{32}$$

The implications of neglecting the cross terms in the evaluation of equations that have the form of equation (32) have been discussed by a number of authors as described by Elishakoff *et al*. (p. 153, reference [16]).

### 5.1. MECHANICAL EXCITATION APPLIED AT A SINGLE POINT

The cross-spectrum of a stationary random force applied at the point $(x_0, y_0)$ is given by (equation (190), reference [4]),

$$S_f(\epsilon_1, \xi_1, \epsilon_2, \xi_2, \omega) = \delta(\epsilon_1 - x_0)\delta(\xi_1 - y_0)\delta(\epsilon_2 - x_0)\delta(\xi_2 - y_0)S_f(\omega), \tag{33}$$

where $S_f(\omega)$ is the force spectral density and $\delta$ is the Dirac delta function. Substituting (33) in (32) and evaluating the double integral one obtains,

$$S_a(x_1, y_1, x_2, y_2, \omega) = \omega^4 \sum_p \frac{\phi_p(x_1, y_1)\phi_p(x_2, y_2)}{\Delta_p^2} \frac{1}{[H_p^2 + W_p^2]} \phi_p^2(x_0, y_0) S_f(\omega). \tag{34}$$

From (34) one can show that the correlation coefficient is given by

$$\gamma_{12}(\mathbf{x}_1, \mathbf{x}_2, \omega) = \frac{\sum_p \phi_p(\mathbf{x}_1)\phi_p(\mathbf{x}_2)\phi_p^2(\mathbf{x}_0)\dfrac{1}{\Delta_p^2[H_p^2 + W_p^2]}}{\left[\sum_p \phi_p^2(\mathbf{x}_1)\phi_p^2(\mathbf{x}_0)\dfrac{1}{\Delta_p^2[H_p^2 + W_p^2]}\right]^{1/2}\left[\sum_p \phi_p^2(\mathbf{x}_2)\phi_p^2(\mathbf{x}_0)\dfrac{1}{\Delta_p^2[H_p^2 + W_p^2]}\right]^{1/2}}, \tag{35}$$

where $\mathbf{x}_1 = (x_1, y_1)$, $\mathbf{x}_2 = (x_2, y_2)$, $\mathbf{x}_0 = (x_0, y_0)$.

The above expression enables the correlation coefficient to be computed for any pair of points and for any frequency. The disadvantage is that one needs to estimate the plate natural frequencies and associated mode shapes. In order to compute a frequency averaged value for the correlation coefficient it is necessary to integrate the term $\Delta_p^2[H_p^2 + W_p^2]$ over frequency. As explained in reference [4], when the natural frequencies $\omega_p$ do not overlap the limits of integration can be extended to infinity. Assuming the modal masses and loss factors are relatively uniform the following standard result is obtained

$$\int_{-\infty}^{\infty} \frac{\mathrm{d}\omega}{\Delta_p^2[(\omega_p^2 - \omega^2)^2 + (\eta_p\,\omega_p\,\omega)^2]} = \frac{\pi}{M^2\eta}, \tag{36}$$

where $M$ is the total mass of the plate and $\eta$ is the plate frequency averaged loss factor. Substituting (36) in (35) one obtains the frequency averaged spatial correlation coefficient of acceleration due to a random point force applied at $\mathbf{x}_0 = (x_0, y_0)$

$$\gamma_{12}(\mathbf{x}_1, \mathbf{x}_2, f_c) = \frac{\sum_p \phi_p(\mathbf{x}_1)\phi_p(\mathbf{x}_2)\phi_p^2(\mathbf{x}_0)}{\left[\sum_p \phi_p^2(\mathbf{x}_1)\phi_p^2(\mathbf{x}_0)\right]^{1/2}\left[\sum_p \phi_p^2(\mathbf{x}_2)\phi_p^2(\mathbf{x}_0)\right]^{1/2}}, \tag{37}$$

where the summation indicated involves all the modes whose natural frequencies are situated inside the frequency band whose centre frequency is $f_c$. This expression is employed in section 6 to obtain theoretical results for the correlation coefficient using modal summation. In the spirit of the approximations employed in this work the modal summation can be substituted by an integration in wavenumber space. As a result the asymptotic form of equation (37) in terms of circular co-ordinates $(k_B, \theta)$ in wavenumber space is given by

$$\gamma_{12}(\mathbf{x}_1, \mathbf{x}_2, f_c) = \frac{\displaystyle\int_{\Delta k}\int_0^{\pi/2} \phi(k_B, \theta, \mathbf{x}_1)\phi(k_B, \theta, \mathbf{x}_2)\phi^2(k_B, \theta, \mathbf{x}_0)\,\mathrm{d}\theta\,\mathrm{d}k_B}{\left[\displaystyle\int_{\Delta k}\int_0^{\pi/2} \phi^2(k_B, \theta, \mathbf{x}_1)\phi^2(k_B, \theta, \mathbf{x}_0)\,\mathrm{d}\theta\,\mathrm{d}k_B\right]^{1/2}\left[\displaystyle\int_{\Delta k}\int_0^{\pi/2} \phi^2(k_B, \theta, \mathbf{x}_2)\phi^2(k_B, \theta, \mathbf{x}_0)\,\mathrm{d}\theta\,\mathrm{d}k_B\right]^{1/2}}, \tag{38}$$

where for a simply supported plate: $\phi(k_B, \theta, \mathbf{x}_1) = \sin(k_B\,x_1\cos\theta)\sin(k_B\,y_1\sin\theta)$. Results from equations (38) and (37) were compared for the case of a simply supported plate:

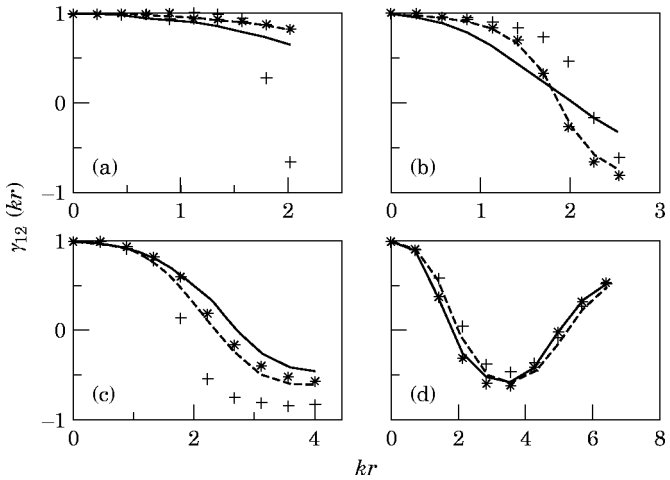


Figure 5. Comparison of results from equation (21) with modal summation results due to point excitation (equation 37). Line D, force at $x = 0{\cdot}165$ m, $y = 0{\cdot}335$ m, one-third octave bands. ——, theory (equation 21); - - - -, large plate (equation 37); + +, small plate (equation 37); **, point excitation (equation 38). (a) 125 Hz; (b) 200 Hz; (c) 500 Hz; (d) 1250 Hz.

examples are presented in section 6. As shown in Figures 5 and 6, good agreement was obtained when the discrete modal summation of expression (37) was computed and compared with the asymptotic results from equation (38). This indicates that expression (38) is a good approximation of the spatial correlation coefficient of point excited structures. This agrees with the analysis of reference [4] (p. 60) in which it is suggested that an asymptotic expression in the form of equation (38) provides an excellent approximation to the exact discrete sum of an equation similar to equation (37). In addition, it is observed that considerations similar to the ones employed in this section will lead to the equation (196) of reference [4].

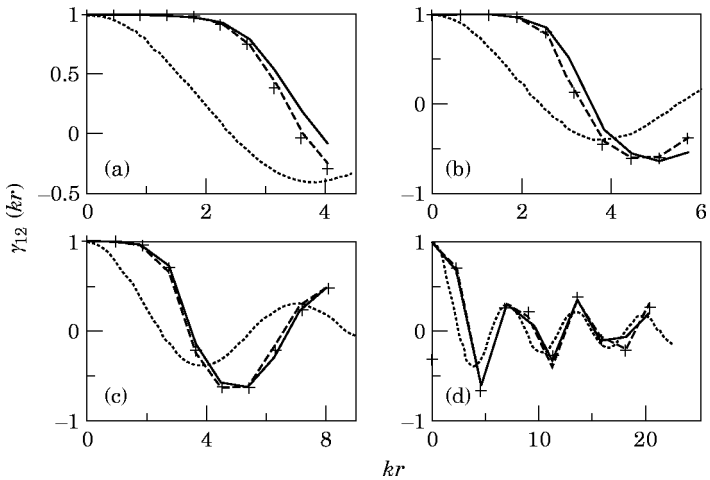


Figure 6. Comparison of results from equation (20) and equation (21) with modal summation results due to point excitation (equation 37). Line B, force at $x = 0{\cdot}24$ m, $y = 0{\cdot}24$ m, one-third octave bands. ——, simply-supported (equation 20); - - - -, large plate, modal sum; + +, point excitation (equation 38); . . . , diffuse field (equation 21). (a) 125 Hz; (b) 250 Hz; (c) 500 Hz; (d) 3150 Hz.

### 5.2. ACOUSTIC EXCITATION IN THE FORM OF A DIFFUSE SOUND FIELD EXCITATION

The cross-spectrum of the random force due to a excitation field in the form of a diffuse acoustic field is given by [17]

$$S_f(\epsilon_1, \xi_1, \epsilon_2, \xi_2, \omega) = (\sin kr/kr)\, S_p(\omega)/2, \tag{39}$$

where $r$ is the distance between points $(\epsilon_1, \xi_1)$ and $(\epsilon_2, \xi_2)$, $k$ is the acoustic wavenumber and $S_p(\omega)$ is the power spectral density of the pressure field. Substituting (39) in (32) one obtains an exact expression for the cross-spectral density of the acceleration response,

$$S_a(x_1, y_1, x_2, y_2, \omega) = \omega^4 \sum_p \frac{\phi_p(x_1, y_1)\phi_p(x_2, y_2)}{\Delta_p^2} \frac{1}{[H_p^2 + W_p^2]} \times \int_S \int_S \frac{\sin kr}{kr} S_p(\omega)\phi_p(\epsilon_1, \xi_1)\phi_p(\epsilon_2, \xi_2)\, \mathrm{d}\epsilon_1\, \mathrm{d}\epsilon_2\, \mathrm{d}\xi_1\, \mathrm{d}\xi_2. \tag{40}$$

where,

$$I_p(\omega) = \int_S \int_S \frac{\sin kr}{kr} S_P(\omega)\phi_p(\epsilon_1, \xi_1)\phi_p(\epsilon_2, \xi_2)\, \mathrm{d}\epsilon_1\, \mathrm{d}\epsilon_2\, \mathrm{d}\xi_1\, \mathrm{d}\xi_2. \tag{41}$$

Assuming the power spectral density of the pressure field varies slowly with frequency and is equal to $S_0$ one can write that

$$S_0\, I_p(\omega) = S_0 \int_S \int_S \frac{\sin kr}{kr} \phi_p(\epsilon_1, \xi_1)\phi_p(\epsilon_2, \xi_2)\, \mathrm{d}\epsilon_1\, \mathrm{d}\epsilon_2\, \mathrm{d}\xi_1\, \mathrm{d}\xi_2. \tag{42}$$

For cases in which the modal mass $\Delta_p$ is almost the same for all the modes, the correlation coefficient due to acoustic excitation in the form of a diffuse acoustic field can be expressed as

$$\gamma_{12}(\mathbf{x}_1, \mathbf{x}_2, \omega) = \frac{\sum_p \phi_p(\mathbf{x}_1)\phi_p(\mathbf{x}_2) \dfrac{I_p(\omega)}{[H_p^2 + W_p^2]}}{\left[\sum_p \phi_p^2(\mathbf{x}_1) \dfrac{I_p(\omega)}{[H_p^2 + W_p^2]}\right]^{1/2} \left[\sum_p \phi_p^2(\mathbf{x}_2) \dfrac{I_p(\omega)}{[H_p^2 + W_p^2]}\right]^{1/2}}. \tag{43}$$

The evaluation of the discrete modal summations presented in the above expression involves computing the plate natural frequencies and associated mode shapes. A frequency averaged result for expression (43) can be derived by following a similar procedure to the one employed for the case of a point excited plate. This expression is

$$\gamma_{12}(\mathbf{x}_1, \mathbf{x}_2, f_c) = \sum_p \phi_p(\mathbf{x}_1)\phi_p(\mathbf{x}_2) I_p(\omega) \Big/ \left[\sum_p \phi_p^2(\mathbf{x}_1) I_p(\omega)\right]^{1/2} \left[\sum_p \phi_p^2(\mathbf{x}_2) I_p(\omega)\right]^{1/2}, \tag{44}$$

where the modes that are included in the summation have resonance frequencies inside the band of interest. The acoustic wavenumber $k$ corresponds to the frequency $f_c$.

Substituting the modal summation by integration in wavenumber space one has, in cylindrical co-ordinates,

$$\gamma_{12}(\mathbf{x}_1, \mathbf{x}_2, f_c) =$$

$$\frac{\displaystyle\int_{\Delta k}\int_{\theta_1}^{\theta_2} \phi(k_B, \theta, \mathbf{x}_1)\phi(k_B, \theta, \mathbf{x}_2) I(k, k_B, \theta)\, \mathrm{d}\theta\, \mathrm{d}k_B}{\left[\displaystyle\int_{\Delta k}\int_{\theta_1}^{\theta_2} \phi^2(k_B, \theta, \mathbf{x}_1) I(k, k_B, \theta)\, \mathrm{d}\theta\, \mathrm{d}k_B\right]^{1/2}\left[\displaystyle\int_{\Delta k}\int_{\theta_1}^{\theta_2} \phi^2(k_B, \theta, \mathbf{x}_2) I(k, k_B, \theta)\, \mathrm{d}\theta\, \mathrm{d}k_B\right]^{1/2}}, \quad (45)$$

where $k$ is calculated for the band centre frequency $f_c$ and

$$I(k, k_B, \theta) = \int_S \int_S \frac{\sin kr}{kr} \phi(k_B, \epsilon_1, \xi_1, \theta)\phi(k_B, \epsilon_2, \xi_2, \theta)\, \mathrm{d}\epsilon_1\, \mathrm{d}\epsilon_2\, \mathrm{d}\xi_1\, \mathrm{d}\xi_2. \quad (46)$$

Following the procedure presented in section 3, for cases in which the bandwidth is not too large, the integral in $k_B$ can be approximated by the expression in the integrand with $k_B$ substituted by the bending wavenumber $k_b$ calculated at the band centre frequency $f_c$.

The limits of integration $\theta_1$ and $\theta_2$ for the case of acoustic excitation are defined by the relative values of the acoustic wavenumber $k$ and the bending wavenumber $k_b$. As explained in reference [18], plate modes which satisfy the condition

$$k_x^2 + k_y^2 < k^2 \quad (47)$$

produce a component that radiates well. By reciprocity, one can suggest that only the plate modes that satisfy the above condition will be efficiently excited by an acoustic field. Therefore, it seems reasonable to evaluate the integral in wavenumber space presented in equation (45) for a region that satisfies the condition (47). From Figure 7 one observes that such a region is situated at the top and bottom ends of the wavenumber quarter-circle. Then if one divides the region of integration into two the following pair of integration limits is obtained,

$$\theta_1' = 0, \qquad \theta_2' = k/k_b\,; \qquad \theta_1'' = \pi/2 - k/k_b, \qquad \theta_2'' = \pi/2; \quad (48)$$

where the first pair correspond to the bottom region and the second pair correspond to the top region. These integration limits were obtained from an approximate analysis of the geometry representation of acoustic and bending wavenumbers on a wavenumber space.

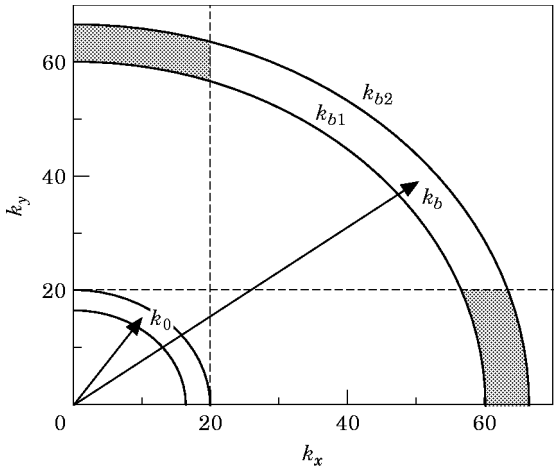


Figure 7. Illustration of wavenumber region with plate modes excited by an acoustic field of wavenumber $k_0$.

In order to obtain a first approximation for the correlation coefficient due to acoustic excitation, the integration limits presented in (48) were used as limits of integration for the standard correlation coefficient expression (equation (30)). It was found that this approximation gave results very similar to ones computed with equation (45). It was also observed that the integration limits employed in the integration of equation (45) do not affect the correlation coefficient results as the multiplication by the factor $I(k, k_b, \theta)$ will have a similar effect to using the integration limits presented in (47).

## 6. SIMPLY SUPPORTED FLAT PLATES: A MODAL SUMMATION APPROACH

A modal summation model that employs the mode shapes of a simply supported flat plate was used to simulate the dynamic behaviour of two simply supported flat plates. The dimensions of these two plates were selected in order that they both have the same bending wavenumber in each frequency band but one has a much higher modal density than the other. The modal summation results are compared with analytical results (equations (20) and (21)) presented in section 3.

The advantages of using a modal summation model are that the number of modal responses summed in each frequency band can be controlled, and the effects of point excitation can be assessed in relation to the spatially uncorrelated excitation (rain-on-the-roof) assumed in the derivation presented in sections 3 and 4. An asymptotic approximation for correlation coefficients on point excited plates is also used in the comparison.

### 6.1. DESCRIPTION OF THE MODAL SUMMATION APPROACH

For a flat plate with simply supported boundary conditions a modal summation expression for the frequency-averaged correlation coefficient of acceleration ($\gamma_{12}(\mathbf{x}_1, \mathbf{x}_2, f_c)$) can be derived from equations (8), (12) and (13). The result is

$$\gamma_{12}(\mathbf{x}_1, \mathbf{x}_2, f_c) = \frac{\sum_N \sin(k_{xM} x_1) \sin(k_{xM} x_2) \sin(k_{yM} y_1) \sin(k_{yM} y_2)}{\left[\sum_N \sin^2(k_{xM} x_1) \sin^2(k_{yM} y_1)\right]^{1/2} \left[\sum_N \sin^2(k_{xM} x_2) \sin^2(k_{yM} y_2)\right]^{1/2}}, \tag{49}$$

where $k_{xM} = m\pi/a$, $k_{yM} = n\pi/b$, $m$ and $n$ are the modal numbers, $a$ and $b$ are the dimensions of the plate in the $x$ and $y$ directions, respectively, and $N$ represents the number of modes summed in each frequency band. The above result presupposes that the excitation is random and spatially uncorrelated.

Based on the above equation the frequency averaged spatial correlation coefficient in each frequency band was estimated in the following way: (i) the plate natural frequencies were calculated and the modes grouped according to frequency band; (ii) the summations presented in equation (49) were then computed for modes whose resonance frequencies are in the respective band; (iii) the summations were repeated for each consecutive pair of points on the line analysed; (iv) the results at each line were then plotted as a function of non-dimensional separation distance $k_b r$ where $k_b$ is the bending wavenumber calculated at the band centre frequency and $r$ is the distance between each pair of points.

### 6.2. DISCUSSION OF RESULTS

The above procedure was employed to estimate the vibration field correlation of two simply supported plates which are illustrated in Figure 8. They both had the same

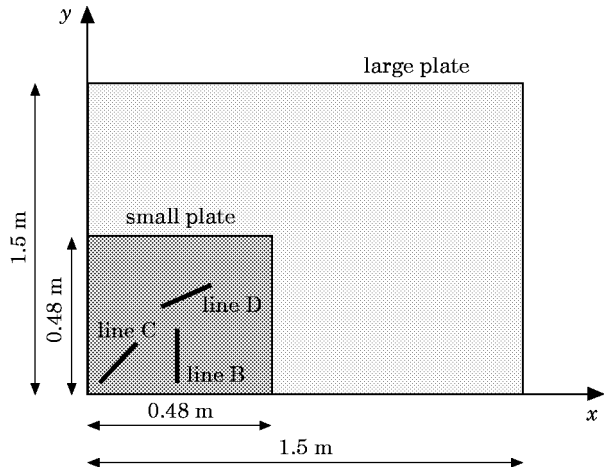


Figure 8. Sketch of lines used in the verification of spatial correlation coefficient results.

thickness, $h = 0{\cdot}001$ m, and were assumed to be made of aluminium. One of the plates had dimensions $a = b = 0{\cdot}48$ m (small plate) and the other $a = b = 1{\cdot}5$ m (large plate). Consequently, both plates had the same bending wavenumber in each frequency band but the large plate had a much higher modal density. In addition, because of the square geometry of both plates, a large number of vibration modes having different shapes but the same natural frequencies were used in the summation.

The correlation coefficient evaluation was carried out for points equally spaced along lines whose positions are indicated in Figure 8. One of the points was assumed fixed and the other displaced from it along the line in nine equally spaced points. Correlation coefficient results were computed for lines B, C and D in one third octave bands from 63 Hz to 3150 Hx and also for 20 frequency bands of constant width of 100 Hz from 50 Hz to 1950 Hz. A large amount of data was obtained in this investigation but only a small selection of significant results are presented here.

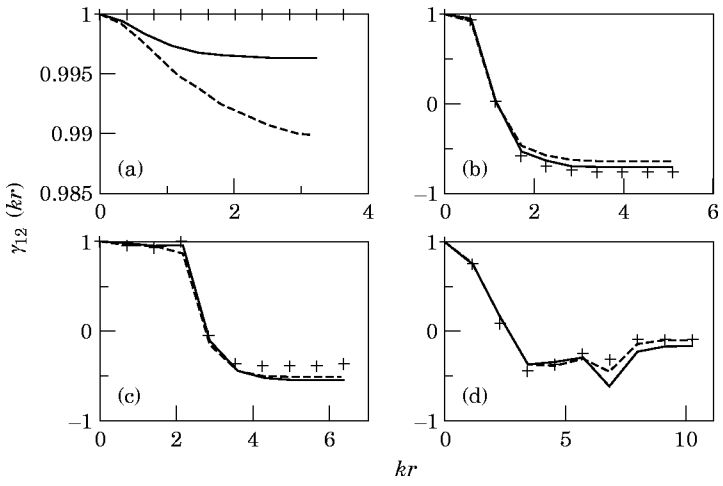


Figure 9. Comparison of results from equation (20) with modal summation results for simply supported plate (equation 49) along line C, one-third octave bands. ——, theory (equation 20); - - - -, large plate (equation 49); + +, small plate (equation 49). (a) 80 Hz, (b) 200 Hz, (c) 315 Hz, (d) 800 Hz.

The comparison between modal summation and analytical results (equation (20)) for points along line C is shown in Figure 9 for some frequency bands. Equal spacing of 2 cm between the points was used on this line. Good agreement was observed between analytical and modal summation results for both plates for frequency bands above (and including) 200 Hz. Results for the small plate did not agree with the theoretical results below 200 Hz because of the small number of modes summed in each 1/3 octave band. For instance, in the 200 Hz one third octave band the number of modes used in the small plate modal summation was five.

As a means of further assessing the number of modes necessary for the analytical frequency averaged results agree with modal summation ones, the modal summation simulation was performed in constant bandwidths of 100 Hz for the small plate. For all the lines the number of modes summed in each band varied from 4 to 8. Results for line C in four frequency bands are presented in Figure 10. For centre frequencies 250 Hz and 450 Hz, six modes were included in the summation, seven modes were summed for 550 Hz band, and only four modes for the 850 Hz frequency band. As shown in Figure 10, when only four modes were included in the summation a poor agreement was observed. A mix of good and reasonable agreement results was obtained for cases when six or seven modes were present in a band. Good agreement was only obtained for cases in which at least eight modes were included in the summation. Similar behaviour was observed for results along the other lines. Stearn [17] employed a similar modal summation procedure to observe that at least ten modes need to be excited at resonance in a frequency band for the correlation coefficient to approximate the diffuse bending wave field function far from the edges of a randomly excited structure. Thus, neglecting the effect of damping, it can be inferred that for bands in which more than eight modes are excited by spatially uncorrelation forces, the modal summation results agree with those of the theoretical model proposed in this work (equation (20)).

The theoretical analysis presented in this work presupposes that the excitation applied to the plate is random and spatially uncorrelated (rain-on-the-roof). Unfortunately, this type of excitation is rarely encountered in real situations because the force is normally applied over a small surface area. The influence of the excitation spatial distribution on the vibration field correlation was analysed using the modal summation model. In the

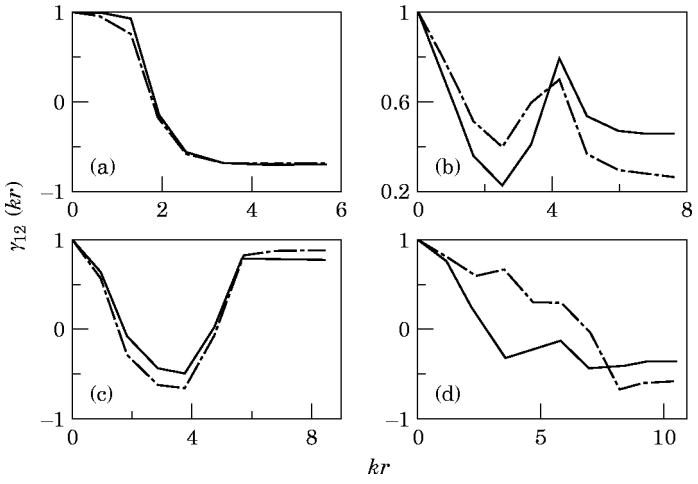


Figure 10. Comparison of results from equation (20) with modal summation results (equation 49) for the small plate along line C, 100 Hz constant bands. Key: ——, theory (equation 20); – · – · –, modal summation (equation 49). (a) 250 Hz (6 modes), (b) 450 Hz (6 modes), (c) 550 Hz (7 modes), (d) 850 Hz (4 modes).

previous section, it was shown that the frequency averaged correlation coefficient due to point excitation at $\mathbf{x}_0 = (x_0, y_0)$ is given by equation (37). The same procedure as that described in section 6.1 was used to obtain the correlation coefficients using equation (37) along the lines sketched in Figure 8. For each line, different positions of the excitation point were used.

A typical result of this simulation is presented in Figure 5. Line D was chosen for this representation as it is reasonably far (in terms of wavelength) from all the boundaries in almost all frequency bands analysed. As expected, it was observed that, along this line, equation (20) (simply-supported flat plate) and equation (21) (two-dimensional diffuse wave field) gave the same results. Thus, only the theoretical results for a simply-supported flat plate (equation (20)) are plotted in Figure 5. The asymptotic expression for the correlation coefficient due to point excitation shown in equation (38) is also employed in this comparison and is labelled 'point excitation' in Figures 5 and 6.

As shown in Figures 5 and 6, results for the large plate and for the asymptotic expression of the point excited correlation coefficient (equation (38)) agreed quite well in the frequency range analysed. Furthermore, both results approached the expression for the spatially uncorrelated correlation coefficient as the frequency increased. Based on modal summation numerical procedure results, Stearn [17] also observed that point excited correlation functions approach that of diffuse bending wave fields for points far (in terms of wavelength) from the edges and excitation point. However, when comparing experimental observations on point excited plates to the diffuse field result, this agreement was not observed. He explained this discrepancy by pointing out that the plates were relatively highly damped.

The relative strengths of the field directly radiated from the point of excitation and the plate reverberant field is strongly dependent on the system damping. An analysis of such relative strength was presented by Skudrzyk [19]. He demonstrated that the distance in which the strength of the field radiated by the point force equals that of the reverberant field is given by (p. 259, reference [19])

$$r = \frac{2\pi l l_0 \eta}{\lambda_B} = l l_0 \eta k_b, \tag{50}$$

where $l$ is the average distance the wave front travels between successive reflections, $l_0$ is the averaged distance to the boundary of the plate, $\eta$ represents the plate loss factor and

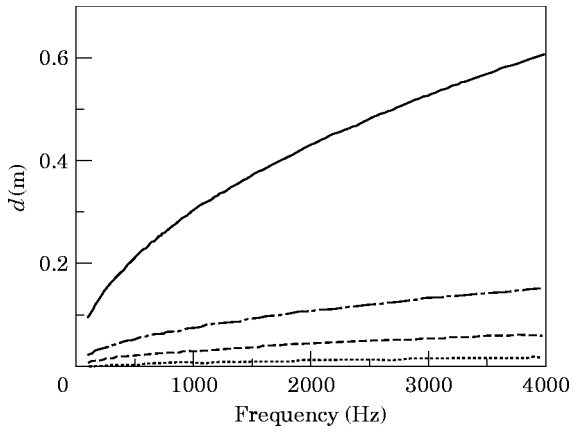


Figure 11. Distance from excitation point at which the strength of the field radiated by the driver equals that of the plate reverberant field as a function of damping. Key: ——, $\eta = 0{\cdot}04$; – · – · –, $\eta = 0{\cdot}01$; - - - -, $\eta = 0{\cdot}004$; · · · · $\eta = 0{\cdot}001$.

$k_b$ is the bending wavenumber. An estimate of this distance for the small plate is presented in Figure 11 as a function of typical loss factors. As shown, for the case of relatively highly damped systems ($\eta > 0{\cdot}04$) the direct field will dominate the vibration field. However, for moderate to low values of loss factor ($\eta < 0{\cdot}01$) the reverberant field will predominate over most of the vibration field, apart from a region very close to the excitation point.

For points close to the system boundaries, such as line B, for which the results are presented in Figure 6, the effect of the point excitation on the vibration field was less pronounced than for points situated far from the edges. This is because the interference field generated by the edges dominates the vibration field in this region. These are only preliminary observations on the influence of the excitation on the correlation coefficients of a vibration field and, as discussed in section 5, further work is necessary to clarify this situation. At present, it can be stated that the theoretical approximations for the correlation coefficient derived in this work can be approximately applied for point excited structures having moderate damping.

Unlike the situation observed for line $D$, the theoretical results from equations (20) and (21) differ considerably for points placed along line $B$. As presented in Figure 6, the zero-crossing points and peak values for results from equation (21) (diffuse bending wave field) are consistently different from that from equation (20) (simply supported flat plate). It was found that, above 400 Hz, both small and large plate results agree with the theoretical results for a simply supported flat plate, whereas results from equation (21) are very different from the other three results in all frequency bands analysed. This disagreement happened irrespective of the type of excitation (spatially uncorrelated or point excitation) and it clearly illustrates the effect of the boundaries in correlating the wave field near the edges.

Furthermore, it was also observed that the relative position of both measurement points in relation to the edges is relevant. In the results presented in Figure 6, one of the points was assumed fixed and placed at the bottom of the line (closer to the edge) and the other moved along the line towards the plate centre. However, were the fixed point placed closer to the centre of the plate, the theoretical formulations (equations (20) and (21)) and modal summation results would be more similar. This indicates that both points need to be placed inside the "one-wavelength-from-the-edges" region for the diffuse wave field and simply-supported results disagree. This observation supports the theoretical analysis of section 3.

## 7. CONCLUSIONS

It is shown that a probabilistic representation can be used to describe the vibration field generated by a structural system based on a spatial correlation model. This probabilistic representation presupposes that a large number of plate modes are available in the frequency band of analysis. The spatial correlation coefficients show large variations in a region one wavelength from the edges; however, in regions more remote from the edges, the form of the spatial correlation is essentially independent of the boundary conditions and approach that of a diffuse bending wave field.

Spatial correlation coefficients for plates subject to point excitation and a diffuse sound field reveal that, due to the normalisation adopted, these coefficients are not much different from those derived for spatially uncorrelated type of excitation. These expressions are restricted to resonant structural response.

Results obtained with the closed form solution derived for the case of a simply supported flat plate are compared to results obtained using a standard modal summation method.

This indicates that at least eight resonant modes need to be included in a frequency band for the present approach be valid. In contradiction to the conclusions of Stearn [17], it is also concluded that a close approximation to a diffuse bending wave field can be set up in a moderately damped, point excited bounded structure.

## ACKNOWLEDGMENT

The financial support of CAPES (Brazilian Government Agency for Postgraduate Education) is here acknowledged.

## REFERENCES

1. G. Maidanik 1962 *Journal of the Acoustical Society of America* **34**, 809–826. Response of ribbed panels to reverberant acoustic fields.
2. M. W. Bonilha 1996 *Ph.D. Thesis*, *University of Southampton*. A hybrid deterministic–probabilistic model for vibroacoustic studies.
3. S. M. Stearn 1971 *Journal of Sound and Vibration* **15**, 353–365. The concentration of dynamic stress in a plate at a sharp change of section.
4. S. H. Crandall 1979 *Developments in Statistics*, *volume* 2 *chapter* 1 (edited by P. R. Krishnaiah). Random Vibration of One- and Two-Dimensional Structures. London: Academic Press.
5. S. H. Crandall 1977 *Stochastic Problems in Dynamics* (edited by B. L. Clarkson, J. K. Hammond, P. J. Holmes, A. Kirstner). Structured Response Patterns due to Wide-Band Random Excitation. London: Pitman.
6. V. V. Bolotin 1984 *Random Vibration of Elastic Systems*. The Hague: Martinus Nijhoff Publishers.
7. S. M. Stearn 1970 *Journal of Sound and Vibration* **12**, 85–97. Spatial variation of stress, strain and acceleration in structures subject to broad frequency band excitation.
8. D. E. Newland 1993 *An Introduction to Random Vibrations*, *Spectral & Wavelet Analysis*. London: Longman; third edition.
9. M. W. Bonilha and F. J. Fahy 1998 *Journal of Sound and Vibration* **214**, 469–496. On the vibration field correlation of randomly excited flat plate structures; II: experimental verification.
10. C. T. Morrow 1971 *Journal of Sound and Vibration* **16**, 29–42. Point-to-point correlation of sound pressures in reverberation chambers.
11. R. H. Lyon 1975 *Statistical Energy Analysis of Dynamical Systems*: *Theory and Applications*. Cambridge, Massachusetts: The MIT Press.
12. R. K. Cook, R. V. Waterhouse, R. D. Berendt, S. Edelman and M. C. Thompson 1955 *Journal of the Acoustical Society of America* **27**, 1072–1077. Measurement of correlation coefficients in reverberant sound fields.
13. S. M. Stearn 1969 *Journal of Sound and Vibration* **9**, 21–27. Measurements of correlation coefficients of acceleration on a randomly excited structure.
14. I. S. Gradshteyn and I. M. Ryzhik 1980 *Table of Integrals*, *Series and Products*. London: Academic Press.
15. R. S. Langley 1991 *Journal of Sound and Vibration* **145**, 261–277. An elastic wave technique for the free vibration analysis of plate assemblies.
16. I. Elishakoff, Y. K. Lin and L. P. Zhu 1994 *Probabilistic and Convex Modelling of Acoustically Excited Structures*. Amsterdam: Elsevier Science.
17. S. M. Stearn 1970 *Ph.D. Thesis*, *University of Southampton*. Stress distributions in randomly excited structures.
18. F. J. Fahy 1985 *Sound and Structural Vibration*: *Radiation*, *Transmission and Response*. London: Academic Press.
19. E. Skudrzyk 1968 *Simple and Complex Vibratory Systems*. University Park, PA: The Pennsylvania State University Press.
20. K. F. Graff 1975 *Wave Motion in Elastic Solids*. New York: Dover.

## APPENDIX A: RESULTS OF SOME INTEGRALS USED IN THIS WORK

$$\int_0^{\pi/2} \cos(A\cos\theta)\,\mathrm{d}\theta = \frac{\pi}{2}\mathrm{J}_0(A), \qquad \text{(reference [14],)} \tag{A1}$$

$$\int_0^{\pi/2} \cos(A\sin\theta)\cos^{2n}\theta\,\mathrm{d}\theta = \frac{\pi}{2}\frac{(2n-1)!}{A^n}\mathrm{J}_n(A), \qquad n > -1/2, \qquad \text{(reference [14],)}$$

then for $n = 0$ one can write that

$$\int_0^{\pi/2} \cos(A\sin\theta)\,\mathrm{d}\theta = \frac{\pi}{2}\mathrm{J}_0(A), \tag{A2}$$

$$I = \int_0^{\pi/2} \cos(A\cos\theta)\cos(B\sin\theta)\,\mathrm{d}\theta = \frac{\pi}{2}\mathrm{J}_0(\sqrt{A^2+B^2}), \qquad \text{(reference [2].)} \tag{A3}$$

## APPENDIX B: DERIVATION OF PARAMETERS OF BOLOTIN'S DYNAMIC EDGE EFFECT METHOD OF MODAL REPRESENTATION FOR VARIOUS BOUNDARY CONDITIONS

Expressions for the spatial correlation coefficient of modally dense flat plates have been derived using an approximate modal representation based on Bolotin's dynamic edge effect method [6]. This representation presupposes that the plate mode shapes remote from the boundaries approaches a sinusoidal function and close to the edges the sinusoidal functions are multiplied by an exponentially decaying function. A typical displacement function is then given by [6]

$$z(x, y, t) = X(x)Y(y)\cos\omega t, \tag{B1}$$

where the functions $X(x)$ and $Y(y)$ change according to the position on the plate and are expressed as

$$X(x) = \sin k_x(x-\xi_x) + C_x\exp(-\mu_x x), \qquad \text{for points close to } x = 0,$$

$$X(x) = \sin k_x(x-\xi_x), \qquad \text{for points remote from } x = 0,$$

$$Y(y) = \sin k_y(y-\xi_y) + C_y\exp(-\mu_y y), \qquad \text{for points close to } y = 0,$$

$$Y(y) = \sin k_y(y-\xi_y), \qquad \text{for points remote from } y = 0.$$

As discussed in sections 3 and 4, the boundary conditions at the edges determine the coefficients $\sin k_x\xi_x$, $\cos k_x\xi_x$, $C_x$, $\sin k_y\xi_y$, $\cos k_y\xi_y$ and $C_y$. In this appendix only coefficients in $x$ are derived, however, the expressions for the coefficients in $y$ are similar, the only modification necessary is to change the indices in $x$ for $y$. Moreover, the wavenumbers $k_x$ and $k_y$ in the expressions shown below are substituted by $k\cos\theta$ and $k\sin\theta$ in the numerical computation.

### B.1. SIMPLY SUPPORTED EDGE

For a left simply supported edge ($x = 0$) one has the following boundary conditions [20] $X(0) = 0$, $X''(0) = 0$. Applying these boundary conditions in the equation for $X(x)$ one has,

$$-\sin k_x\xi_x + C_x = 0, \qquad k_x^2\sin k_x\xi_x + \mu_x^2 C_x = 0.$$

The solution of the above system of equations is given by,

$$\sin k_x \xi_x = C_x = 0, \tag{B2}$$

and as a result,

$$\cos k_x \xi_x = 1. \tag{B3}$$

B.2. CLAMPED EDGE

The boundary conditions on a left clamped edge ($x = 0$) are given by $X(0) = X'(0) = 0$. Applying these boundary conditions in equation (B1) one obtains the following system of equations,

$$\sin k_x \xi_x = C_x, \qquad \cos k_x \xi_x = (\mu_x / k_x) C_x.$$

Solving this system of equations one obtains

$$C_x = \sin k_x \xi_x = \frac{k_x}{\sqrt{2(k_x^2 + k_y^2)}}, \qquad \cos k_x \xi_x = \frac{\mu_x}{\sqrt{2(k_x^2 + k_y^2)}} = \frac{\sqrt{k_x^2 + 2k_y^2}}{\sqrt{2(k_x^2 + k_y^2)}}. \tag{B4}$$

B.3. FREE EDGE

For a left free edge ($x = 0$) one has that [20]

$$\partial^2 z/\partial x^2 + v\, \partial^2 z/\partial y^2 = \partial^3 z/\partial x^3 + (2 - v)\, \partial^3 z/\partial x\, \partial y^2 = 0.$$

Applying these boundary conditions in equation (B1), including evanescent terms for $X(x)$ but neglecting evanescent terms for $Y(y)$, the following system of equations is obtained

$$(k_x^2 + v k_y^2) \sin k_x \xi_x + (\mu_x^2 - v k_y^2) C_x = 0,$$

$$(k_x^3 + (2 - v) k_x k_y^2) \cos k_x \xi_x + (\mu_x^3 - (2 - v) \mu_x k_y^2) C_x = 0.$$

The solution of this system of equations is given by,

$$\sin k_x \xi_x = |W_1| / \sqrt{W_1^2 + W_2^2}, \tag{B5}$$

$$\cos k_x \xi_x = |W_2| / \sqrt{W_1^2 + W_2^2}, \qquad C_x = 1 / \sqrt{W_1^2 + W_2^2}, \tag{B6, B7}$$

where,

$$W_1 = -\frac{(\mu_x^2 - v k_y^2)}{(k_x^2 + v k_y^2)}, \qquad W_2 = -\frac{(\mu_x^3 - (2 - v) \mu_x k_y^2)}{(k_x^3 + (2 - v) k_x k_y^2)}.$$

B.4. GUIDED EDGE

The following boundary conditions apply for a left guided edge ($x = 0$),

$$X'(0) = X'''(0) = 0.$$

In a similar manner to the previous cases, one can apply these boundary conditions to equation (B1) and obtain,

$$k_x \cos k_x \xi_x - \mu_x C_x = 0, \qquad k_x^3 \cos k_x \xi_x + \mu_x^3 C_x = 0.$$

The solution of the above system of equations is given by,

$$\cos k_x \xi_x = C_x = 0, \tag{B8}$$

and as a result,

$$\sin k_x \xi_x = 1. \tag{B9}$$

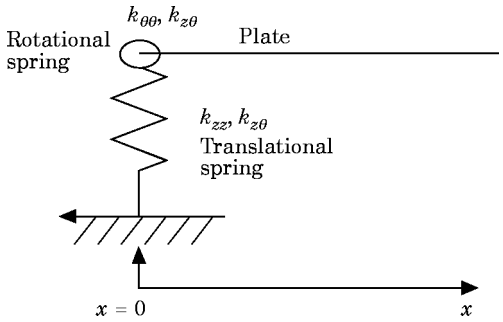


Figure B1. General spring attachment along the left edge of a plate.

## B.5. GENERAL SPRING ATTACHMENT

As a means of deriving the coefficients for a general type of edge attachment the plate is assumed to be uniformly supported along the edge by a translational and a rotational spring. This support provides translational, rotational and coupling resistance and the respective stiffness are $k_{zz}$, $k_{\theta\theta}$ and $k_{z\theta}$. A sketch of this support is presented in Figure B1. For a left edge (x = 0) the equations associated with this type of support are given by,

$$D\left[\frac{\partial^3 z}{\partial x^3} + (2-\nu)\frac{\partial^3 z}{\partial y^2\,\partial x}\right] = k_{zz}\,z + k_{z\theta}\left(\frac{\partial z}{\partial x}\right), \qquad -D\left[\frac{\partial^2 z}{\partial x^2} + \nu\frac{\partial^2 z}{\partial y^2}\right] = k_{\theta\theta}\left(\frac{\partial z}{\partial x}\right) + k_{z\theta}\,z.$$

Applying these boundary conditions in equation (B1), including evanescent terms for $X(x)$ but neglecting evanescent terms for $Y(y)$, one obtains the following system of equations,

$$(-Dk_x^3 - Dk_x k_y^2(2-\nu) - k_{z\theta}k_x)\cos k_x\xi_x + k_{zz}\sin k_x\xi_x$$
$$+(-D\mu_x^3 + D(2-\nu)\mu_x k_y^2 - k_{zz} + k_{z\theta}\mu_x)C_x = 0,$$
$$(Dk_x^2 + Dk_y^2\nu - k_{z\theta})\sin k_x\xi_x + k_{\theta\theta}k_x\cos k_x\xi_x + (D\mu_x^2 - Dk_y^2\nu - k_{\theta\theta}\mu_x + k_{z\theta})C_x = 0.$$

The solution of the above system of equations yields,

$$\sin k_x\xi_x = (W_2W_4 - W_3W_5)/\sqrt{(W_1W_5 - W_6W_2)^2 + (W_2W_4 - W_3W_5)^2}, \quad \text{(B10)}$$

$$\cos k_x\xi_x = (W_1W_5 - W_6W_2)/\sqrt{(W_1W_5 - W_6W_2)^2 + (W_2W_4 - W_3W_5)^2}, \quad \text{(B11)}$$

$$C_x = (W_3W_6 - W_1W_4)/\sqrt{(W_1W_5 - W_6W_2)^2 + (W_2W_4 - W_3W_5)^2}, \quad \text{(B12)}$$

where,

$$W_1 = Dk_x^2 + Dk_y^2\nu - k_{z\theta}, \qquad W_2 = D\mu_x^2 - Dk_y^2\nu - k_{\theta\theta}\mu_x + k_{z\theta}, \qquad W_3 = k_{\theta\theta}k_x,$$
$$W_4 = -Dk_x^3 - Dk_xk_y^2(2-\nu) - k_{z\theta}k_x, \qquad W_5 = -D\mu_x^3 + D(2-\nu)\mu_xk_y^2 - k_{zz} + k_{z\theta}\mu_x,$$
$$W_6 = k_{zz}.$$

## B.6. STIFFNESS COEFFICIENTS FOR A BEAM/STIFFENER COUPLING [15]

The parameters of the Bolotin's dynamic edge effect method can be applied to beam/stiffener coupling. It is only necessary to express the stiffness coefficients $k_{zz}$, $k_{\theta\theta}$ and $k_{z\theta}$ as a function of the stiffener dynamic properties. The stiffness coefficients of a general stiffener (illustrated in Figure B2) have been considered in reference [15] and were derived in the form

$$k_{zz} = EI_1k_2^4 - \rho A\omega^2, \qquad k_{z\theta} = -EI_{12}c_0k_2^4 - \rho Ac_2\omega^2,$$

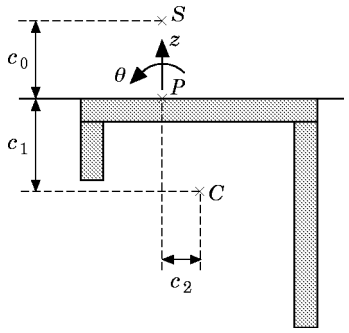


Figure B2. Geometry of stiffener [15].

$$k_{\theta\theta} = (E\Gamma + EI_2\, c_0^2)k_2^4 + GJk_2^2 - (I + \rho A c_1^2 + \rho A c_2^2)\omega^2, \tag{B13}$$

where $EI_1$, $EI_2$ and $EI_{12}$ are the flexural rigidities of the stiffener, $E\Gamma$ and $GJ$ are the torsional rigidities, $\rho A$ are the mass and polar moment of inertia per unit length. The points S, C and P in Figure B2 represent the shear centre, the centroid and the plate attachment point, respectively. The stiffness coefficients presented in (B13) were derived assuming the plate is effectively rigid in-plane ($k_L$ and $k_s = 0$).